Seismic Performance of Steel Plate Shear Walls Considering Two Different Design Philosophies of Infill Plates. II: Assessment of Collapse Potential

Ronny Purba, Ph.D., A.M.ASCE[1]; and Michel Bruneau, Ph.D., P.Eng., F.ASCE[2]

Abstract: Assessment of collapse potential and seismic performance was conducted for steel plate shear walls (SPSWs) having infill plates designed per two different philosophies. This assessment was first conducted on SPSWs that were designed neglecting the contribution of their boundary moment resisting frames to resist story shear forces. This assessment of collapse potential was repeated for SPSWs that were designed considering the sharing of story shear forces between the boundary frames and infill plates. Based on these assessments, seismic performance factors [i.e., response modification coefficient (R-factor), system overstrength Ω_0 factor, and deflection amplification C_d factor] for both types of SPSWs were identified and compared. Adjustments to improve collapse performance and factors that affect collapse potential were presented. Collapse fragility curves for archetypes with various structural configurations (i.e., panel aspect ratio, intensity level of seismic weight, and number of stories) were investigated. Findings from these analyses demonstrate that the infill plates of SPSWs should be designed to resist the total specified story shears, and that SPSWs designed by sharing these story shears between the boundary frame and infill plates will undergo significantly larger and possibly unacceptable drifts. **DOI: 10.1061/(ASCE)ST.1943-541X.0001097.**

Author keywords: Seismic performance; Steel plate shear walls; Infill plates design; Collapse potential; Collapse fragility curves; Seismic performance factors; FEMA P695 methodology; Seismic effects.

Introduction

Current building codes for the design of steel plate shear walls (SPSWs) [AISC 2010; Canadian Standards Association (CSA) 2009] are ambiguous regarding whether the contribution of the boundary frame moment resisting action to the global plastic lateral strength of SPSWs can be taken into account regarding resisting lateral loads, or whether the infill plates of SPSWs must be designed to resist the complete lateral loads. In the latter case, the seismic behavior of SPSWs has traditionally benefited from the overstrength introduced in the horizontal and vertical boundary elements (HBE and VBEs), but questions have arisen in recent years suggesting that explicitly allowing sharing of lateral loads between the boundary frame and infill plates as a means to optimize SPSW designs might be cost-effective; however, consequences on behavior are unknown (Qu and Bruneau 2009; Bhowmick et al. 2011). Based on their experiences designing multistory SPSWs, researchers have assigned a certain percentage of the total design base shear to be resisted by the boundary frame and the remaining portion resisted by the infill plates. Other researchers, however, developed a procedure to design SPSWs considering boundary frame moment resisting action to theoretically achieve a balanced (optimum) design minimizing overstrength of the system. Both design approaches use the same response modification coefficient (i.e., R-factor) as that of conventional SPSWs, implicitly assuming that both types of SPSWs may feature comparable seismic performances. Qu and Bruneau (2009) commented on the possible need to design the optimized systems with a different R-factor, based on limited results showing that SPSWs designed to have lateral loads shared by infill plates and boundary frame experienced larger drifts than conventional SPSWs.

This paper investigates the seismic performance of SPSWs having infill plates designed per these two different philosophies. Using the FEMA P695 methodology (2009), which defines the performance in terms of collapse potential under maximum considered earthquake (MCE) ground motions, the assessment is first conducted on SPSWs that are designed neglecting the contribution of their boundary moment resisting frames to resist story shear forces. In other words, infill plates are designed to resist the entire story shear forces. This assessment of collapse potential is repeated for SPSWs that are designed considering the sharing of story shear forces between the boundary frames and infill plates. Based on these assessments, seismic performance factors [i.e., response modification coefficient (R-factor), system overstrength Ω_0 factor, and deflection amplification C_d factor] for both types of SPSWs are identified and compared.

One key element of the assessment specified in the FEMA P695 methodology (2009), which is the development of accurate structural models to simulate the component strength deterioration, has been addressed in a companion paper (Purba and Bruneau 2014b). Building on the results reported in the companion paper, this paper presents the steps and results of seismic performance assessments including the development of SPSW archetypes, the formulation of nonlinear analytical model, the results of nonlinear static and dynamic analyses (i.e., pushover and incremental dynamic analyses), and the evaluation of collapse performance. Adjustments to improve collapse performance and factors that affect collapse potential are presented, along with collapse fragility curves for

[1]Instructor, Dept. of Civil Engineering, Univ. of Minnesota, 121 Swenson Civil Engineering, 1405 University Dr., Duluth Campus, Duluth, MN 55812 (corresponding author). E-mail: rhpurba@d.umn.edu

[2]Professor, Dept. of CSEE, Univ. at Buffalo, 130 Ketter Hall, Buffalo, NY 14260. E-mail: bruneau@buffalo.edu

Note. This manuscript was submitted on September 19, 2013; approved on April 10, 2014; published online on August 5, 2014. Discussion period open until January 5, 2015; separate discussions must be submitted for individual papers. This paper is part of the ***Journal of Structural Engineering***, © ASCE, ISSN 0733-9445/04014161(12)/$25.00.

Table 1. Story Weight and Design Base Shear of SPSW Archetypes

Archetype[a]	Level	W_{SPSW} (kips)	$W_{P\text{-}\Delta}$ (kips)	W_{total} (kips)	V_d (kips)
SW310, SW310K	Roof	63.42	317.41	380.83	154.84
	Lower	58.61	292.99	351.60	
SW320, SW320K	Roof	126.94	253.89	380.83	175.87
	Lower	117.20	234.40	351.60	
SW320KR6	Roof	126.94	253.89	380.83	205.18
	Lower	117.20	234.40	351.60	
SW320KR5	Roof	126.94	253.89	380.83	246.22
	Lower	117.20	234.40	351.60	
SW320G, SW320GK	Roof	126.94	1,014.55	1,141.49	464.51
	Lower	117.20	937.83	1,055.03	
SW520, SW520K	Roof	126.94	253.89	380.83	255.32
	Lower	117.20	234.40	351.60	
SW520G, SW520GK	Roof	126.94	1,014.55	1,141.49	765.95
	Lower	117.20	937.83	1,055.03	
SW1020, SW1020K	Roof	136.00	256.30	392.30	680.88
	Lower	126.25	237.93	364.18	

Note: V_{total} = design base shear; $W_{P\text{-}\Delta}$ = gravity loads on P-Δ leaning column; W_{SPSW} = gravity loads on SPSW; W_{total} = total seismic weight for base shear calculation (= $W_{SPSW} + W_{P\text{-}\Delta}$).
[a]Convention follows the following example, SW320GKR6 = steel walls; three story archetype; aspect ratio 2.0; high tributary seismic mass (high gravity loads on leaning column); design with $\kappa_{balanced}$; design with R-factor of 6 instead of 7.

archetypes having various structural configurations (i.e., panel aspect ratio, intensity level of seismic weight, and number of stories).

Development of Steel Plate Shear Wall Archetypes

SPSW archetypes were designed either for the case in which the infill plates alone can resist 100% of the specified seismic load without considering boundary frame moment resistance (conventional design with $\kappa = 1.0$) or for the case in which SPSWs are optimized to effectively eliminate overstrength (as a consequence of the boundary frame strength) such that the sum of the strength of boundary frame and infill plates was exactly equal to the required strength to resist the designed lateral loads. This optimum design was defined as the balanced design case (i.e., $\kappa = \kappa_{balanced}$) by Qu and Bruneau (2009). Here, the percentage of shear forces resisted by the infill plate for balanced design case was estimated as follows:

$$\kappa_{balanced\_i} = \left[1 + \frac{1}{2}\tan^{-1}(\alpha_i)\left(\frac{L}{h_i}\right)\right]^{-1} \quad (1)$$

where α = tension field inclination angle; L and h = width and height of the panel, respectively. All parameters correspond to the properties at the ith story.

For the purpose of quantifying seismic performance factors for SPSWs having infill plates designed to sustain different levels of lateral loads, 12 SPSW archetypes consisting of three to 10 story office buildings were prepared (i.e., six archetypes each for conventional and balanced design cases). For convenience, their loading information, floor plans, and elevations were as assumed to be similar to the SAC model building described in FEMA 355-C (2000). Each SPSW archetype was designed to have one bay width, 3.96 m (13 ft) story height, and low to moderate aspect ratio (i.e., aspect ratio of either 1.0 or 2.0). To avoid unnecessary overstrength, the required infill plate thickness to resist story shear forces was assumed to be available, and varied along the height of the building as a function of story shear force demands. All SPSWs had moment resisting HBE-to-VBE connections.

The total number of 12 archetypes developed here is less than that specified for a complete application of the FEMA P695 procedure (i.e., 48 archetypes). In this research, however, selected archetypes were investigated that represent critical SPSW configurations. Both design approaches used the capacity design principle outlined in the AISC seismic provisions (2010) to design HBEs and VBEs; archetypes were explicitly designed to avoid the development of in-span hinges, per the design procedure addressed by Purba and Bruneau (2012). Two levels of seismic tributary weight were considered: low and high seismic weights. Here, for a specified design seismic load, fewer numbers of SPSWs present in a building correspond to high seismic tributary weight for each SPSW and vice versa. Archetypes were sized based on the design basis earthquake (DBE) response spectra specified in FEMA P695 (2009) for high seismicity [i.e., seismic design category (SDC) D_{max}]. Story seismic weight and design base shear for each archetype are listed in Table 1. In selecting the VBE and HBE sections, an optimum design objective with a demand-to-capacity ratio close to 1.0 (without exceeding it) was exercised. The resulting sizes of VBEs, HBEs, and infill plate are summarized in Table 2 for the three-story archetypes, whereas those for the five-story and 10-story archetypes can be found in Purba and Bruneau (2014a).

Nonlinear Models for Collapse Simulation

Fig. 1 shows an example two-dimensional nonlinear model for collapse simulation of three-story SPSW archetypes developed in *OpenSees*. This dual strip model incorporates an axial hinge at every strip and concentrated fiber plastic hinges (each with 65 fibers across the cross section) at the ends of VBEs and HBEs.

Table 2. Design Summary of Three-Story SPSW Archetypes for Collapse Assessment

SPSW components	100% design case ($\kappa = 1.0$)			Balanced design case ($\kappa = \kappa_{balanced}$)[a]		
	SW310	SW320	SW320G	SW310K	SW320K	SW320GK
HBE-3	W14 × 53 (1.0)[b]	W18 × 76 (0.99)	W27 × 146 (0.96)	W12 × 40 (0.95)	W18 × 40 (0.99)	W21 × 93 (0.96)
HBE-2	W12 × 45 (0.99)	W14 × 61 (0.99)	W14 × 159 (0.96)	W10 × 33 (0.95)	W12 × 35 (0.98)	W18 × 71 (0.97)
HBE-1	W16 × 31 (0.98)	W12 × 45 (0.95)	W18 × 97 (0.97)	W12 × 22 (0.94)	W10 × 26 (0.95)	W14 × 48 (1.0)
HBE-0	W18 × 86 (0.94)	W24 × 117 (0.98)	W24 × 306 (0.97)	W18 × 55 (0.96)	W21 × 68 (0.98)	W21 × 166 (0.98)
VBE-3	W18 × 50 (0.96)	W16 × 89 (0.98)	W27 × 161 (0.98)	W16 × 36 (0.98)	W14 × 53 (0.94)	W14 × 132 (0.99)
VBE-2	W18 × 71 (0.98)	W18 × 76 (0.99)	W27 × 178 (0.95)	W16 × 45 (0.96)	W18 × 40 (0.98)	W21 × 93 (0.96)
VBE-1	W21 × 122 (1.0)	W24 × 146 (0.96)	W36 × 300 (1.0)	W18 × 86 (0.96)	W24 × 76 (0.96)	W21 × 201 (0.97)
t_{w3} [mm (in.)]	1.8034 (0.071)	0.9144 (0.036)	2.5654 (0.101)	1.1176 (0.044)	0.4572 (0.018)	1.1938 (0.047)
t_{w2} [mm (in.)]	2.921 (0.115)	1.4986 (0.059)	4.1402 (0.163)	1.8034 (0.071)	0.7366 (0.029)	1.9812 (0.078)
t_{w1} [mm (in.)]	3.5814 (0.141)	1.8288 (0.072)	5.1562 (0.203)	2.2098 (0.087)	0.889 (0.035)	2.3876 (0.094)

[a]Balanced condition: $\kappa_{balanced} = 0.63$; $L/h = 1.0$; $\alpha_{average} = 41°$ (SW310K); $\kappa_{balanced} = 0.49$; $L/h = 2.0$; $\alpha_{average} = 44°$ (SW320K, SW320GK).
[b]Value in parentheses is demand-to-capacity ratio.

Panel zones are not included in this model because their impacts on the global behavior of the model are insignificant. Deterioration material models for SPSW components (i.e., strips and boundary elements) have been presented in a companion paper [Fig. 8 in Purba and Bruneau (2014b)]. The "gravity-leaning-column" elements are added adjacent to the strip model. These columns are not part of the lateral force resisting system, but their presence is necessary to capture the destabilizing effects from the gravity load assigned to the columns (as is common in nonlinear analysis considering P-Δ effects). The values of gravity loads located on the SPSW and the leaning column for each archetype are summarized in Table 1. Although these are classically called "leaning columns" in P-Δ analysis, the columns themselves have no initial physical leaning at the start of the analysis.

In *OpenSees*, the leaning column was modeled by using an elastic beam-column (EBC) element. Typically with this approach, the cross-sectional area of the EBC element is multiplied by the number of gravity columns present in the structure. However, because there is no definitive information on the number of gravity columns in the archetypes, the cross-sectional area is arbitrarily increased by 100 times the value of one column to represent the aggregate effect of all gravity columns; this is of no significance to the results because the column axial deformations are not a concern in this study. By contrast, the moment of inertia was designated as 100 times smaller than the likely moment of inertia of one column to simulate a moment release at both ends of the EBC element (i.e., pin-ended element); this is required to ensure that the gravity columns do not contribute to lateral load resistance while accounting for P-Δ effects. Rigid links were used to connect the leaning column and SPSWs at every floor; these were modeled by using a truss element with cross-sectional area arbitrarily increased to 100 times the HBE cross section at the corresponding floor. No seismic mass was applied on the leaning column; all were applied to an SPSW and distributed equally to its left and right joints at every story.

Application of FEMA P695 Methodology to Three-Story SPSW Archetypes

Structural System Archetypes and Uncertainty Factors

The following illustrates how the FEMA P695 methodology (2009) was applied to all archetypes under consideration by using two three-story SPSW archetypes. The archetypes SW320 and SW320K, selected for this purpose, are representative of the two basic SPSW configurations considered in this research: the design of SPSWs with κ factor equal to 1.0 and the balanced design case with κ factor set to be $\kappa_{balanced}$, respectively. As summarized in Table 1, both SW320 and SW320K archetypes were designed to resist a design base shear of 782.8 kN (176 kips). However, the amount of base shear resisted by their infill plates was different. In SW320, the entire specified design base shear was resisted by its infill plates, whereas for SW320K, the infill plates only resisted 382.5 kN (86 kips) and the remaining base shear of 400.3 kN (90 kips) was resisted by its boundary frame. Incidentally, the calculation of design base shear according to the FEMA P695 methodology (2009) is based on theoretical fundamental periods rather than analytical fundamental periods. Although both archetypes theoretically have the same period of 0.36 s, their analytical fundamental periods are slightly different (i.e., 0.35 and 0.50 s for SW320 and SW320K, respectively). However, because both are in the constant acceleration region of the design spectra, the design base shear is the same for either case.

For the purpose of performance evaluation, uncertainty factors related to archetypes and nonlinear model must be determined by rating the design procedures used to size the archetypes, the experimental data used to verify the proposed strength degradation model, and the collapse modes incorporated in the nonlinear model (Fig. 1) according to the guidelines described in the FEMA P695 (2009) methodology. The following paragraphs briefly describe how these were assessed.

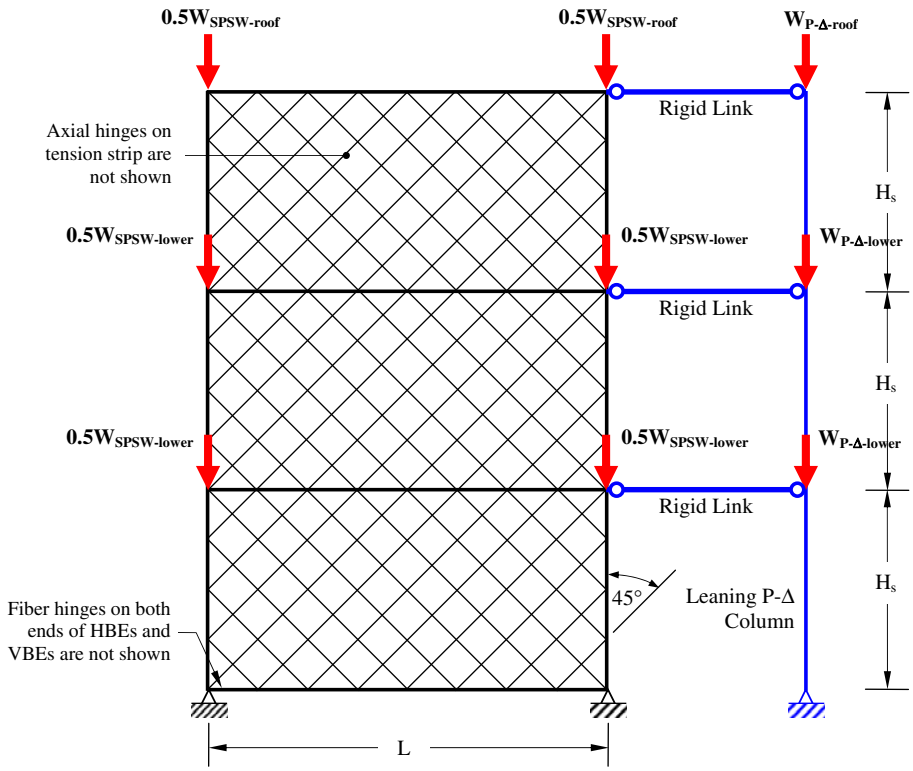

Fig. 1. Nonlinear model for collapse simulation: example structural model of three-story archetype

Uncertainty related to design requirements: In this research, the procedures used to design SPSW archetypes followed the current design procedures described in the AISC seismic provisions (2010) for SPSW. Developed based on SPSW research conducted in the last 30 years, this provision provides sufficient design requirements to safeguard against unanticipated failure modes. Moreover, SPSWs have been implemented in several low-rise and high-rise buildings as their primary lateral-force resisting systems [examples are provided by Bruneau et al. (2011)]. However, no documented performance is available of SPSWs during earthquakes (at the time of this writing) to verify whether a well-designed SPSW actually performed as intended. Hence, based on the FEMA P695 guidelines (2009), the current SPSW design requirements are rated as B (good) and the corresponding uncertainty related to design requirements (β_{DR}) equals 0.2. Over time, as research on SPSW continues and new understanding is gained of SPSW behavior, this value may be revisited.

Uncertainty related to test data: At the time of this writing, 36 conventional unstiffened slender-web SPSWs have been tested by various researchers (Purba and Bruneau 2014b). This total number of tested SPSW specimens is relatively low in comparison with that of other lateral-force-resisting systems (e.g., special moment frames). In addition, all SPSW specimens tests focused on investigating the global behavior of the system and there is a lack of individual component tests. Hence, SPSW test data at the time of this writing is rated as C (fair) and the corresponding uncertainty related to test data (β_{TD}) equals 0.35.

Uncertainty related to nonlinear model: Based on past SPSW experimental research available at the time of this writing, common deterioration and failure modes in steel plate shear walls have been identified and addressed in Purba and Bruneau (2014b). Among the identified failure modes, two primary factors that may contribute to the collapse of SPSWs (i.e., deteriorating web tearing and flexural failure of boundary elements) were considered in the development of nonlinear models used in this research [Fig. 8 in Purba and Bruneau (2014b)]. However, the deteriorated material models were calibrated only to a limited number of SPSW specimens that have stable strength degradation behavior. Hence, the nonlinear analytical model developed in this research is rated as B (good) and the corresponding uncertainty related to nonlinear model (β_{MDL}) equals 0.2.

Nonlinear Pushover Analysis and Incremental Dynamic Analysis

Nonlinear pushover analysis is performed to estimate system overstrength (Ω_o) and period-based ductility (μ_T) factors for both archetypes. These factors are defined as follows:

$$\Omega_o = \frac{V_{\max}}{V}; \qquad \mu_T = \frac{\delta_u}{\delta_{y,\text{eff}}} \tag{2}$$

where $V_{\max}$ and V = maximum and design base shear strength for a given archetype model, respectively; δ_u and $\delta_{y,\text{eff}}$ = ultimate and effective yield roof displacement of the archetype model, respectively. The μ_T factor is later used for the performance evaluation. As shown in Fig. 2, the ultimate base shear strengths for SW320 and SW320K are 2201.8 and 1005.2 kN (495 and 226 kips), respectively. Hence, Ω_o factors are 2.8 and 1.3 for the respective archetypes. Moreover, $\delta_{y,\text{eff}}$ and δ_u for SW320 are 45.7 and 226.1 mm (1.8 and 8.9 in.), respectively, while for SW320K, the respective values are 45.7 and 218.4 mm (1.8 and 8.6 in.) Hence, μ_T factors are 4.9 and 4.8 for SW320 and SW320K, respectively. Although both archetypes have significantly different

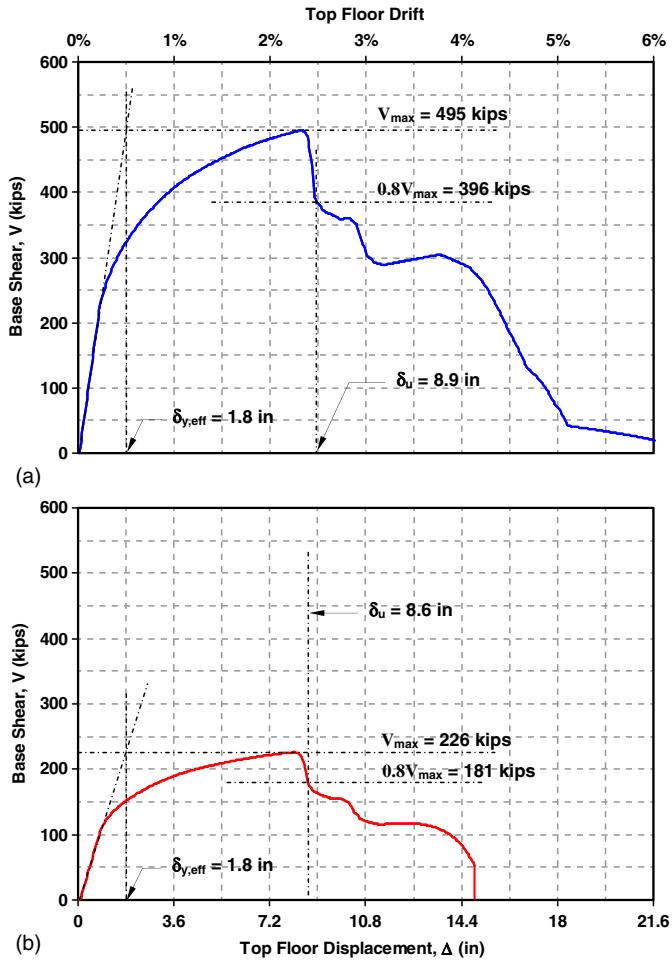

Fig. 2. Monotonic pushover analysis results: (a) SW320; (b) SW320K

strength capacities, they have slightly similar displacement capacities.

Incremental dynamic analysis (IDA) was performed to determine median collapse capacity, $\hat{S}_{CT}$, and collapse margin ratio (CMR). The CMR is defined as follows:

$$\text{CMR} = \frac{\hat{S}_{CT}}{S_{MT}} \tag{3}$$

where S_{MT} = response spectrum of MCE ground motions at the fundamental period of a given archetype. The ground motion records used consisted of 22 far-field ground motion record pairs (44 individual components) of large magnitude ($M > 6.5$) from sites located at distances greater than or equal to 10 km from fault rupture [Pacific Earthquake Engineering Research Center (PEER) 2005].

Fig. 3 presents IDA results and the corresponding collapse fragility curves for SW320 and SW320K. The median collapse spectral acceleration intensity, $\hat{S}_{CT}$, is 3.6 and 2.3 g for SW320 and SW320K, respectively. These results indicate that at the same level of 50% collapse probability, the spectral acceleration intensity at which 22 ground motions caused the collapse of SW320 is higher than that which caused SW320K to collapse. The collapse fragility curves also indicate that when both archetypes are subjected to a set of ground motions having their median spectral acceleration scaled to the MCE response spectra level of 1.5 g, SW320K has a higher probability of collapse than SW320. In this case, the collapse

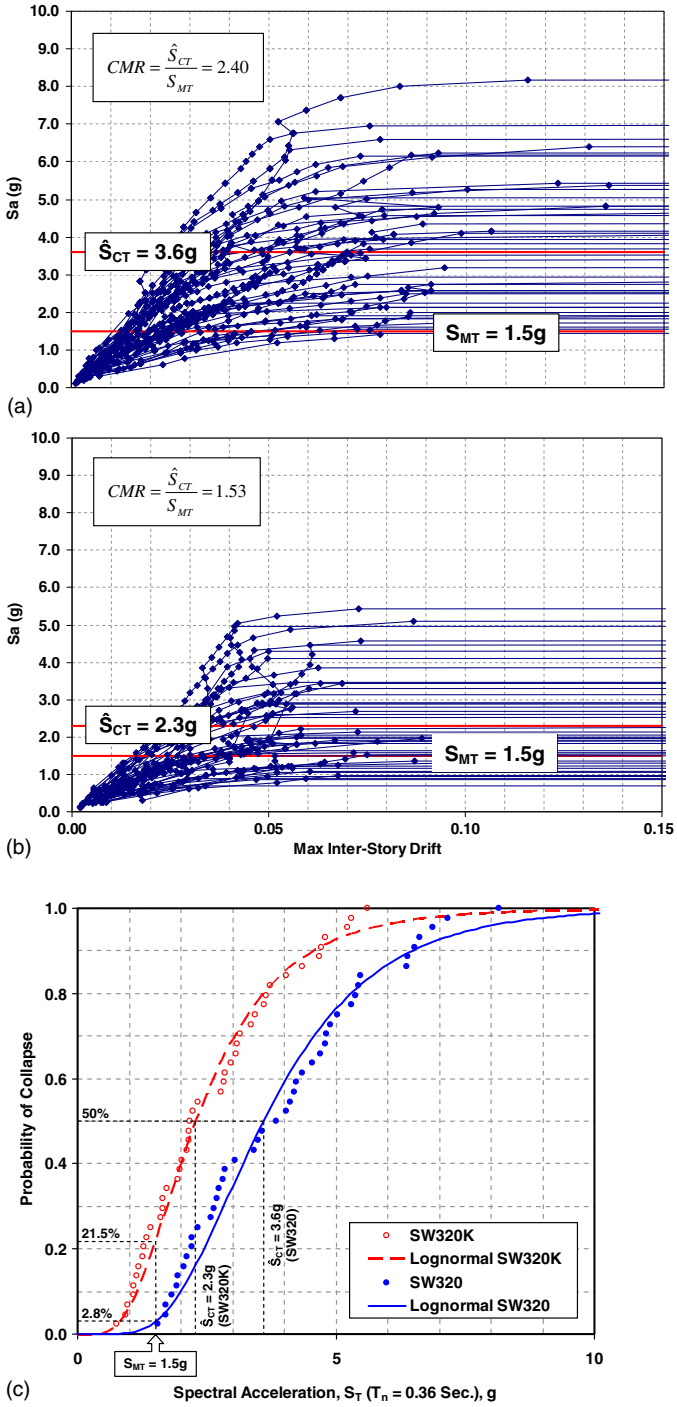

Fig. 3. IDA results: (a) SW320; (b) SW320K; (c) collapse fragility curves for SW320 and SW320K

probabilities at the MCE level are 21.5 versus 2.8% for SW320K and SW320, respectively. The same information is also indicated by the IDA curves, in which more collapses (i.e., flat lines) occur below the S_{MT} level for the SW320K case than for SW320. Here, the CMR values are 2.4 and 1.5 for SW320 and SW320K, respectively.

Collapse Performance Evaluation

The performance evaluation starts by adjusting the CMR value determined from the IDA to consider the frequency content of the selected ground motion records (i.e., the effect of spectral shape). Spectral shape factor (SSF) values used to modify the CMR to the adjusted collapse margin ratio (ACMR) are functions of the archetype fundamental period (T) and μ_T factor determined from the pushover analysis. The analytical fundamental period calculated using the FEMA P695 procedures (2009) is 0.36 s for both archetypes. For T less than 0.5 s, μ_T values of approximately 5, and seismic design category (SCD) D_{max}, the value of SSF [determined from a table provided in FEMA P695 (2009)] is approximately 1.25 for both archetypes. Accordingly, the ACMR values for SW320 and SW320K are 3.0 and 1.9, respectively. These values will be compared to preestablished acceptable ACMR values to justify whether the initial R-factor used to design these archetypes satisfies the FEMA P695 requirements (2009).

To estimate acceptable ACMR, total system collapse uncertainty (β_{TOT}) is required. The value of β_{TOT} is obtained by combining uncertainty factors related to record-to-record (β_{RTR}), design requirements (β_{DR}), test data (β_{TD}), and nonlinear modeling (β_{MDL})

$$\beta_{TOT} = \sqrt{\beta_{RTR}^2 + \beta_{DR}^2 + \beta_{TD}^2 + \beta_{MDL}^2} \tag{4}$$

For the selected ground motions used in the FEMA P695 (2009) methodology, a constant value of β_{RTR} equal to 0.4 is used, given that period-based ductility is larger than or equal to 3 ($\mu_T \geq 3$). The other three uncertainty factors have been presented previously (i.e., β_{DR}, β_{TD}, and β_{MDL} values are 0.2, 0.35, and 0.2, respectively). Hence, β_{TOT} is 0.6. According to a table provided in FEMA P695 (2009), the acceptable ACMR for 10% collapse probability under MCE ground motions (i.e., $ACMR_{10\%}$) for β_{TOT} of 0.6 is 2.16. Here, SW320 passes the FEMA requirement (i.e., ACMR of 3.0 is larger than $ACMR_{10\%}$ of 2.16), but SW320K does not (i.e., ACMR of 1.9 is smaller than $ACMR_{10\%}$ of 2.16).

Seismic Performance Factors for Steel Plate Shear Walls

The preceding procedure was repeated for all archetypes under consideration; their performance evaluations are summarized in Table 3. Detailed information is provided by Purba and Bruneau (2014a). All conventional archetypes passed the performance criterion. The computed ACMR for each archetype was larger than the acceptable $ACMR_{10\%}$ of 2.16. These results indicate that each archetype has a reasonable safety margin against collapse (i.e., a lower probability of collapse) as a result of the overstrength reserve provided by the boundary frame. For this type of SPSW, results indicate that the R-factor of 7 used in design is adequate (i.e., satisfied the ACMR requirement). The Ω_o factor for the archetypes (based on the pushover analysis results) varied from 2.3 to 3.1. Considering the limited numbers of SPSW archetypes designed in this research, the Ω_o factor of 2.0 can be considered adequate for conventional SPSW. Assuming the inherent damping available in SPSW to be 5% of critical damping, a C_d factor of 7 can be considered for conventional SPSWs. The resulting seismic performance factors for conventional SPSWs determined in this case are similar to those specified in ASCE 7-10 (2010) (i.e., R, Ω_o, and C_d factors are 7, 2, and 6, respectively).

For the balanced archetypes, except for the 10-story archetype and five-story archetype design with high seismic weight (i.e., SW1020K and SW520GK), no other archetypes met the performance criterion because their computed ACMR was smaller than $ACMR_{10\%}$. These results indicate that the R-factor of 7 used in the initial step to design the balanced SPSW does not lead to an adequate design (i.e., the result did not satisfy the ACMR

Table 3. Summary of Performance Evaluation for SPSW Archetypes with Various Structural Configurations

	Pushover results						IDA results		Performance evaluation		
Archetype	V_d (kips)	V_{max} (kips)	$\delta_{y,eff}$ [mm (in.)]	δ_u [mm (in.)]	$\Omega_0 = V_d/V_{max}$	$\mu_T = \delta_u/\delta_{y,eff}$	$\hat{S}_{CT}$ (g)	CMR $= \hat{S}_{CT}/S_{MT}$	SSF[a]	ACMR[b]	Pass/fail[c]
SW310	155	401	53.34 (2.1)	297.18 (11.7)	2.6	5.5	3.14	2.10	1.26	2.64	Pass
SW320	176	495	45.72 (1.8)	226.06 (8.9)	2.8	4.9	3.60	2.40	1.25	3.00	Pass
SW320G	465	1,440	45.72 (1.8)	251.46 (9.9)	3.1	5.5	4.08	2.72	1.26	3.43	Pass
SW520	255	578	99.06 (3.9)	414.02 (16.3)	2.3	4.2	3.40	2.42	1.25	3.03	Pass
SW520G	766	1,924	104.14 (4.1)	495.3 (19.5)	2.5	4.8	4.26	3.03	1.27	3.85	Pass
SW1020	681	1,975	198.12 (7.8)	1031.24 (40.6)	2.9	5.2	3.40	4.08	1.36	5.58	Pass
SW310K	155	236	53.34 (2.1)	266.7 (10.5)	1.5	5.0	2.28	1.52	1.25	1.90	Fail
SW320K	176	226	45.72 (1.8)	218.44 (8.6)	1.3	4.8	2.29	1.53	1.24	1.90	Fail
SW320GK	465	618	43.18 (1.7)	226.06 (8.9)	1.3	5.1	2.32	1.55	1.25	1.93	Fail
SW520K	255	254	96.52 (3.8)	408.94 (16.1)	1.0	4.3	2.10	1.50	1.25	1.80	Fail
SW520GK	766	837	96.52 (3.8)	454.66 (17.9)	1.1	4.7	2.64	1.88	1.27	2.39	Pass
SW1020K	681	953	200.66 (7.9)	1043.94 (41.1)	1.4	5.2	1.92	2.30	1.36	3.16	Pass
SW320KR6	205	270	43.18 (1.7)	218.44 (8.6)	1.3	5.0	2.47	1.65	1.25	2.06	Fail
SW320KR5	246	334	45.72 (1.8)	231.14 (9.1)	1.4	5.1	2.87	1.91	1.25	2.39	Pass

[a]SSF obtained from FEMA P695 (2009) table for given T and μ_T.
[b]ACMR $=$ SSF$(T, \mu_T) \times$ CMR; $S_{MT} = 1.5$, 1.4, and 0.83 g for three-story, five-story, and 10-story archetypes, respectively.
[c]Acceptance criteria: $ACMR_{10\%}$ for β_{TOT} of 0.6 $= 2.16$; pass if ACMR $\geq ACMR_{10\%}$, otherwise fail.

requirement). Design iterations are required to determine acceptable seismic performance factors for SPSW designed with $\kappa_{balanced}$.

Adjustments to Satisfy Collapse Performance of Balanced Archetypes

Three possible adjustments can be applied to improve collapse performance of the balanced archetypes: (1) reducing the β_{TOT}; (2) accepting a higher probability of collapse; and (3) designing the balanced archetypes with a lower value of R-factor. In the first two adjustments, basically, the demand for the balanced archetypes to satisfy the collapse performance criterion is lowered, whereas in the last adjustment, the capacity of the balanced archetypes is increased.

First Adjustment: Reducing System Collapse Uncertainty Factor

The performance chart shown in Fig. 4 is used to illustrate the first adjustment. This performance chart shows acceptable ACMR for different levels of collapse probabilities and β_{TOT}. The value shown in the middle of each cell is the acceptable ACMR for a given collapse probability and total system collapse uncertainty. A linear interpolation can be applied to determine acceptable ACMR for a condition between two levels of β_{TOT}. One example is the current β_{TOT} of 0.6, which is between good (B) and fair (C). For β_{TOT} of 0.6 and collapse probability of 10%, the previous $ACMR_{10\%}$ of 2.16 can be determined from a linear interpolation between 2.53 and 1.96. For a given performance evaluation, a star-shaped marker is located above the thick gray line if a calculated ACMR is higher than an acceptable ACMR, otherwise the marker is located below the thick gray line. The thick gray line constitutes a less than 5% difference between the calculated and acceptable ACMRs. As shown in this performance chart, lower total system collapse uncertainty and higher allowed collapse probability result in lower acceptable ACMR.

The calculated ACMR for balanced archetypes (e.g., SW320K) was 1.90, which was lower than the $ACMR_{10\%}$ of 2.16. This condition is indicated in the performance chart by the star marker labeled 1. To reduce β_{TOT}, hypothetically, one may optimistically rate the current SPSW design requirements, currently available SPSW experimental data, and the nonlinear model developed to model SPSW as A (superior, $\beta_{DR} = 0.1$), B (good, $\beta_{TD} = 0.2$), and B (good, $\beta_{MDL} = 0.2$), respectively, for resulting β_{TOT} of 0.5. As a result of the smaller collapse uncertainty, for the same collapse probability of 10%, the resulting $ACMR_{10\%}$ are 1.90, obtained from a linear interpolation of the values in the performance chart between 1.78 (superior, A) and 1.96 (good, B) for β_{TOT} of 0.5. Hence, the performance point moves from star markers 1 to 2, which now satisfies the performance criterion.

However, adjusting uncertainty factors by selecting lower values is rather subjective. The current uncertainty factors selected for this research were deemed appropriate considering the current understanding of SPSW behavior. As more research on SPSW becomes

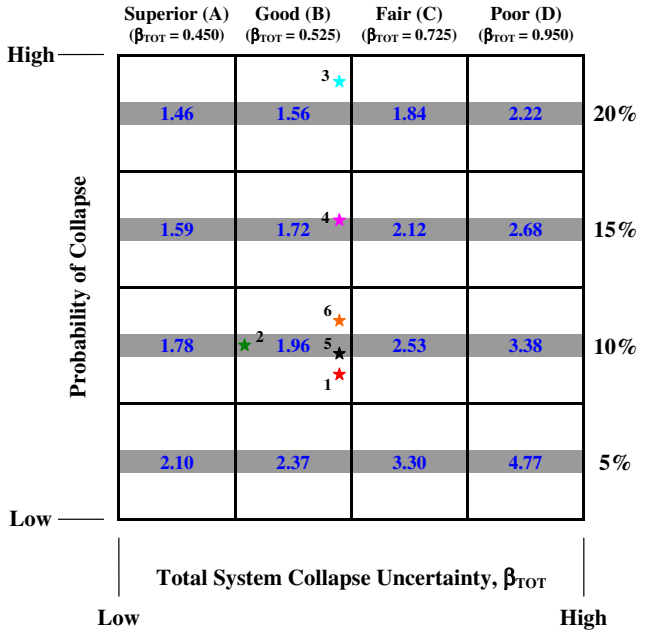

Fig. 4. Performance chart: acceptable ACMR for specific probability of collapse and total system uncertainty

available, expert opinions may determine whether lower uncertainty factors for SPSW are acceptable. Hence, the preceding theoretical adjustment is only presented here for illustration purposes, to show the potential benefits to improving knowledge on the collapse performance of balanced archetypes.

Second Adjustment: Accepting Higher Probability of Collapse

The second possible adjustment is to accept a higher probability of collapse. If a collapse probability of 20% is considered acceptable and the same level of total system collapse uncertainty of 0.6 is selected, the threshold value for the balanced archetypes (i.e., $ACMR_{20\%}$) reduces to 1.66. In this case, the performance point in the performance chart (Fig. 4) moves from star-marker 1 to 3, which satisfies the performance criterion. However, according to the FEMA P695 methodology (2009), doing so would be acceptable only if many more archetypes were designed such they can be grouped into several performance groups with at least three archetypes in each performance group. Alternatively, one may select different acceptable collapse probability values (for example, 15%, which would provide $ACMR_{15\%} = 1.86$ for $\beta_{TOT} = 0.6$) to satisfy the performance criterion (i.e., indicated by star-marker 4). Again, expert opinions would be required to determine an appropriate level of collapse probability for SPSW other than that currently specified in the FEMA P695 methodology (2009).

Third Adjustment: Designing Balanced Archetypes with Lower R-Factors

The third possible adjustment to improve the collapse performance of balanced archetypes is to design them with a lower value of the *R*-factor and repeat the performance evaluation with the same collapse probability of 10% and β_{TOT} of 0.6. Here, this was achieved by designing another three-story balanced archetype with *R*-factor of 6. This archetype was denoted as SW320KR6.

The resulting collapse fragility curve for SW320KR6 determined from IDA is plotted in Fig. 5, superposed with the fragility curves for SW320 and SW320K. Interestingly, contrary to initial expectations, reducing the *R*-factor from 7 to 6 did not result in a significant improvement in the collapse margin ratio. The CMR for SW320KR6 is 1.65, which is approximately an 8% increase from that of SW320K.

The performance evaluation for SW320KR6 is summarized in Table 3. Compared with the results for SW320K, SW320KR6 shows a slight improvement in period-based ductility, a similar system overstrength, and a slight increase in the calculated ACMR. The calculated ACMR of 2.06 is approximately 5% below the acceptable $ACMR_{10\%}$ of 2.16 (i.e., indicated by star-marker 5 in Fig. 4). Although some may consider this difference acceptable, to be rigorous, another design iteration was performed by using an *R*-factor of 5; the resulting balanced archetype is denoted as SW320KR5. The IDA results and performance evaluation for this archetype are also presented in Fig. 5 and Table 3. As hoped, SW320KR5 satisfied the performance criteria. Here, the calculated ACMR of 2.39 is 11% higher than the threshold $ACMR_{10\%}$ (i.e., indicated by star-marker 6).

For completeness, the same iteration process with *R*-factor lower than 7 should be conducted on the other balanced archetypes that did not satisfy the performance criterion (i.e., SW310K, SW320GK, and SW520K). Considering that these archetypes have practically the same ACMR as SW320K with *R*-factor of 7, it was assumed that comparable results to that of SW320KR5 would be achieved if these archetypes were designed with *R*-factor of 5.

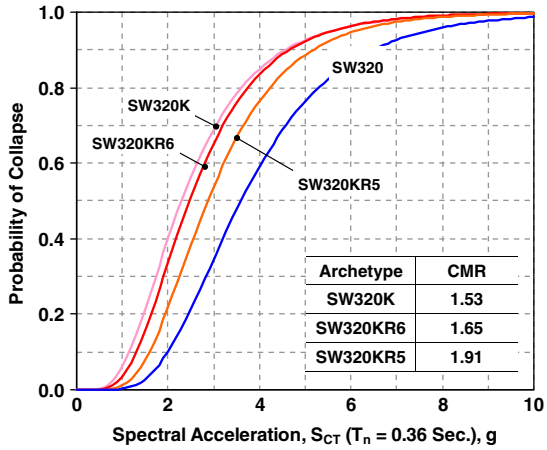

Fig. 5. Fragility curves for archetypes with different *R*-factors

Hence, such redesigns were not attempted, and the *R*-factor of 5 was deemed adequate for all balanced cases.

Based on these results, seismic performance factors for SPSW designed with $\kappa_{balanced}$ are recommended to be smaller than those for conventional SPSW (i.e., the 100% design case, $\kappa = 1.0$). Results indicate that an *R*-factor of 5 should be used for the design of balanced SPSWs. No system overstrength factor is available in balanced SPSWs (i.e., $\Omega_o = 1$). As with conventional SPSWs, the C_d factor for balanced SPSWs should be similar to the assigned *R*-factor (i.e., $C_d = 5.0$).

Interstory Drift as Damage Measure

The damage measure (DM) is a parameter used in IDA to characterize the responses of archetypes under specified ground motions (Vamvatsikos and Cornell 2002). The collapse point at which excessive lateral interstory displacement occurred in the archetypes is typically selected as a DM. However, in general, the collapse point of an archetype occurs at a considerably large interstory drift. For example, the median interstory drifts (i.e., corresponding to 50% probability of exceedance) when collapse occurred in SW320 and SW320K are 7.6 and 5.8%, respectively.

Considering these results, it is also meaningful to interpret the IDA results in terms of drift demands. Specifically, fragility curves can be constructed for the probability of exceeding certain drift values in terms of spectral acceleration of the ground motions, for selected fixed values of interstory drifts up to the drift at the collapse. The resulting drift-exceedance fragility curves for SW320 and SW320K, using interstory drifts as DMs, are plotted in Figs. 6(a and b), respectively. As a reference, the results from Fig. 3 using the collapse point as the DM are superimposed in these curves. At the MCE level (i.e., $S_{MT} = 1.5$ g), there is an approximately 50% probability that drifts will exceed 2 and 3.5% interstory drifts for SW320 and SW320K, respectively. More significantly, at a 20% probability of exceedance, the respective archetypes will exceed 3 and 7% interstory drifts. The results indicate that SW320K has a higher probability of suffering significant larger interstory drift, which can be associated with larger structural and nonstructural damages. The same results were also obtained when comparing SW1020 and SW1020K in Figs. 6(c and d). For the conventional archetype, half of the ground motions resulted in approximately 2% interstory drift, whereas those for the balance archetype resulted in 3% interstory drift. At a 20% probability of exceedance, the respective 10-story archetypes will exceed 2.5 and 4.5% interstory drifts.

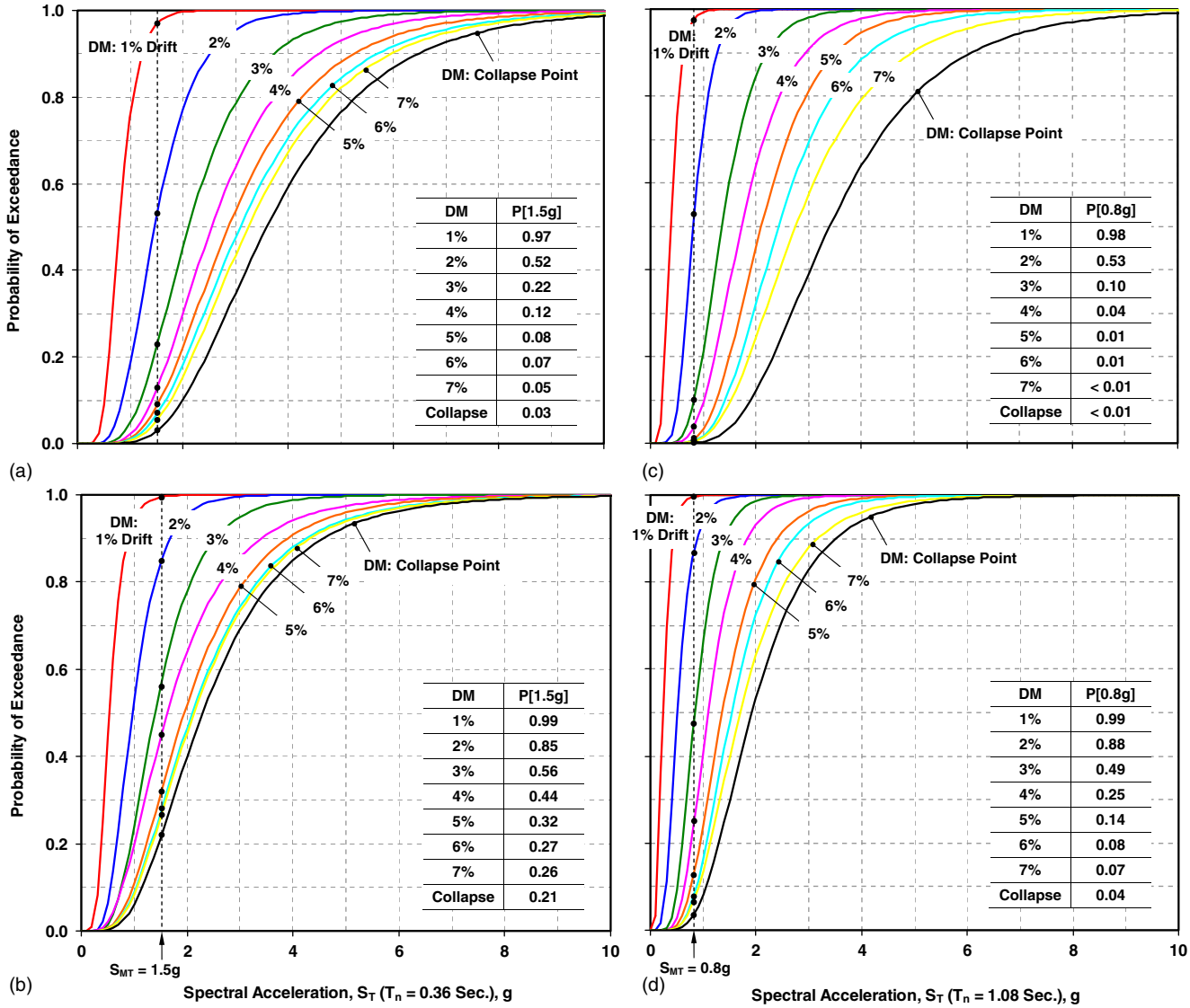

Fig. 6. Exceedance fragility curves using various level of interstory drift as damage measure: (a) SW320; (b) SW320K; (c) SW1020; (d) SW1020K

Although the calculated ACMR of the 10-story balanced archetype (i.e., SW1020K) met the acceptable ACMR limit, its probability to undergo a significantly large interstory drift (i.e., ≥3%) can be as high as 50% under MCE ground motions (Fig. 6). Whereas this SPSW designed with a balanced case and *R*-factor of 7 has a sufficient margin to collapse, its ability to prevent damage to the structure and to drift-sensitive nonstructural components is significantly less than for its counterpart archetype (i.e., SW1020). Hence, the need to design balanced archetypes with smaller *R*-factor is deemed necessary.

In terms of the probability of exceeding the damage measures of 2, 3, and 4% interstory drift, results indicate that reducing the *R*-factor from 7 to 6 resulted in an improvement of exceedance probability of no more than 10% for SW320KR6 compared to SW320K. More specifically, whereas half of the ground motions under consideration at the MCE level resulted in approximately 3.5% interstory drifts for SW320K, this slightly improved to 3.0% interstory drifts for SW320KR6. Moreover, half of the ground motions under consideration at the MCE level caused approximately 2.5% maximum interstory drifts for SW320KR5, which is tolerable and closer to that expected for conventional SPSWs.

In terms of the total steel weight for archetypes designed with different *R*-factors, the reference conventional SPSW [i.e., SW320, designed per AISC (2010) with an *R*-factor of 7] requires a total of 4,744 kg (10,459 lb) of steel. The case designed with $\kappa_{balanced}$ with *R*-factor of 7, SW320K, requires a total of 2.602 kg (5,737 lb) of steel, which is approximately 55% less than that required for the conventional design; however, as indicated previously, SW320K did not meet the collapse performance criterion according to the FEMA P695 (2009) methodology and a lower *R*-factor must be used. Designed with *R*-factors of 6 and 5, SW320KR6 and SW320KR5 require 17 and 31% more steel than SW320K, but SW320KR5 still provides a 28% reduction in the total weight of steel from that required for the conventional SPSW. However, this savings in steel comes at the cost of the SPSW designed for $\kappa_{balanced}$ developing larger interstory drifts than the conventional SPSWs (i.e., 2.5 versus 2.0% interstory drift) under MCE ground motions.

Impact of Archetype Configurations on Collapse Margin Ratio

In addition, the results for the preceding 12 SPSW archetypes were compared to investigate variations in collapse performance for

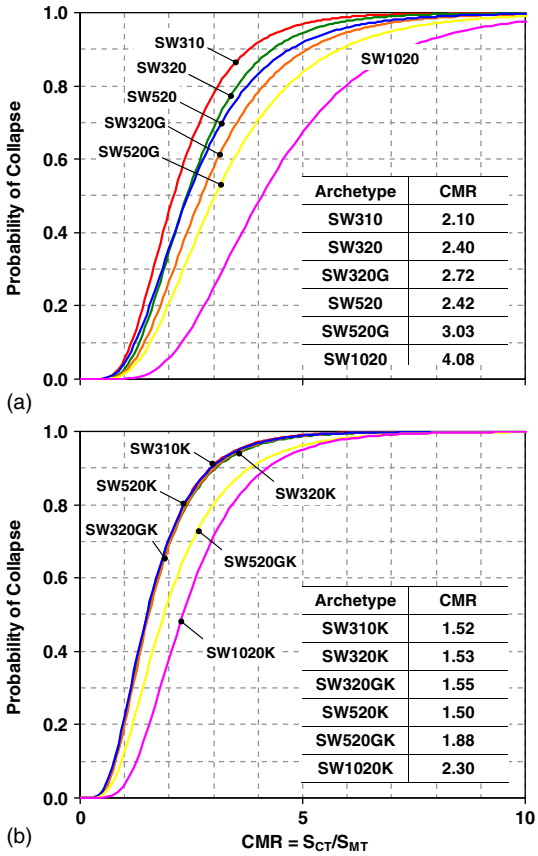

Fig. 7. Collapse fragility curves for archetypes with various configurations: (a) 100% design case; (b) balanced design case

various structural configurations. This section presents collapse fragility curves for these archetypes and compares collapse margin ratios for archetypes with different panel aspect ratio, intensity of active seismic weight, and number of stories. The resulting collapse fragility curves and the corresponding collapse margin ratios are presented in Fig. 7.

Panel Aspect Ratio

To observe the impact of panel aspect ratio on collapse margin ratios, collapse fragility curves for SW310 and SW310K were compared to that of the benchmark archetypes SW320 and SW320K, respectively. As shown in Fig. 7(a) for the conventional design case ($\kappa = 1$), CMR for SW310 (i.e., a three-story archetype with panel aspect ratio of 1.0) is 2.10, which is 12.5% smaller than that of SW320 (i.e., a three-story archetype with panel aspect ratio of 2.0). This CMR for archetypes with smaller panel aspect ratio is reasonable in light of the information reported by Qu and Bruneau (2009) as presented in Fig. 8, which shows that overstrength decreases as panel aspect ratio decreases. In other words, as a consequence of less overstrength present in SW310 than in SW320, its probability of collapse under MCE ground motions is higher (i.e., its margin to collapse is smaller). However, the 12.5% CMR difference between SW310 and SW320 is rather small, considering the large difference in overstrength between the two archetypes shown in Fig. 8. Here, for the case in which the κ factor equals 1.0, a 25% overstrength difference theoretically exists between these archetypes. This indicates that, although Fig. 8 provides insights into the relative magnitude of CMRs between archetypes having different aspect ratios, the relationship between overstrength and CMR values is not necessary linearly correlated.

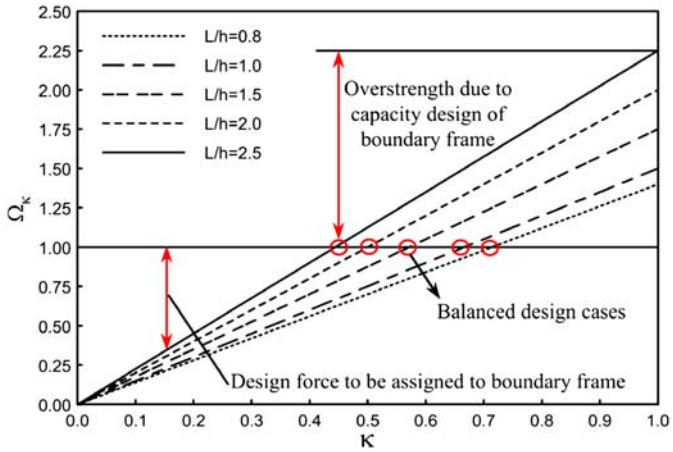

Fig. 8. Relationship between $\Omega\kappa$ and κ for various aspect ratios (Qu and Bruneau 2009, ©ASCE)

By contrast, the balanced archetypes (i.e., SW310K versus SW320K) have practically similar margins to collapse. As shown in Fig. 7(b), their collapse fragility curves are on top of each other and their respective CMR values are 1.52 and 1.53. This result may be expected, considering that both archetypes have the same minimum amount of overstrength.

Intensity Level of Seismic Weight

Two intensity levels of seismic weight were considered: low and high seismic weight. SPSW archetypes in the former category (e.g., SW320, SW320K, SW520, and SW520K) were designed to sustain tributary seismic weight equal to one-sixth of the total story seismic weight in the selected prototype buildings (i.e., the SAC model buildings); those in the latter category (e.g., SW320G, SW320GK, SW520G, and SW520GK) were designed to sustain half of the total story seismic weight. The terms "low" and "high" seismic weight can be interpreted to correspond to the cases termed low and high gravity loads in FEMA P695 (2009), respectively, assigned to the gravity leaning column system (P-Δ column). Distribution of gravity loads assigned to VBEs and gravity leaning columns is presented in Table 1 for all archetypes under consideration.

Initially, it was suspected that archetypes designed with high seismic weight would have lower (or, at worst, similar) margins to collapse than those with low seismic weight. This hypothesis was founded on the idea that the fundamental period of both archetypes would be comparable because the ratio between their structural masses and stiffness would be similar (i.e., archetypes with low seismic weight would have smaller component sizes and lower stiffness, whereas those with high seismic weight would have bigger component sizes and higher stiffness). Indeed, calculations confirmed that the fundamental periods of archetypes designed with high and low seismic weights, for the same number of stories, were similar. Accordingly, their responses under one particular ground motion were expected to be comparable at a lower level of earthquake excitations. However, for the case in which gravity loads on the leaning columns are considerably larger, P-Δ effects may cause archetypes designed with high seismic weight to reach collapse sooner than those with low seismic weight. On that basis, five-story archetypes were expected to possibly have smaller CMR compared to three-story archetypes, because P-Δ effects would be more pronounced in higher buildings.

Interestingly, contrary to the initial expectation, the archetypes designed with higher seismic weight were found to actually have

higher CMR values. This result can be observed in all cases under consideration (Fig. 7). Specifically, the conventional three-story archetype, SW320G (designed with high seismic weight), has a 13% higher CMR than SW320 (designed with low seismic weight). The difference is even higher for the conventional five-story archetypes, in which the CMR of SW520G (equal to 3.03) is 25% higher than that of SW520. For the balanced three-story archetypes, however, the difference between CMR values of archetypes designed with high and low seismic weight was insignificant, with CMR values for SW320GK and SW320K of 1.55 and 1.53, respectively. Differing from these results, the CMR of SW520GK (i.e., balanced five-story archetype designed with high seismic weight) was 25% higher than the CMR of its counterpart archetype, SW520K, designed with low seismic weight (a difference similar to that observed for the conventional five-story archetypes).

As a first attempt to comprehend the cause for the preceding trends, the intensity of each ground motion that caused the three-story archetype designed with high seismic weight to collapse (S_{CT}) was compared to the ground motion intensity that caused the same for the three-story archetype designed with low seismic weight. For the conventional archetypes (i.e., between SW320G and SW320), most ratios are larger than 1.0 (i.e., for 41 ground motions), which means that the majority of ground motions have to be scaled up to a higher intensity to cause the collapse of SW320G as opposed to that of SW320. By contrast, for the balanced archetypes (i.e., between SW320K and SW320K), the intensity ratios larger and smaller than 1.0 are comparable (i.e., 26 ground motions caused the collapse of SW320GK at a higher intensity than for SW320K, and 18 at a lower intensity). These results were the same for the five-story archetypes.

Although the preceding provides some statistical quantification supporting the observation of higher CMR for archetypes designed with high seismic weight (because CMR is linearly correlated to the median collapse intensity of the 44 ground motions), further investigation is required to understand the actual reason for the aforementioned trends. For this purpose, a series of monotonic pushover analyses was conducted to investigate the impact of P-Δ columns and deteriorated material models on archetypes designed with high and low seismic weights. The analyses were conducted on the three-story and five-story archetypes and on the conventional and balanced design archetypes (i.e., a total of eight archetypes).

In the first set of analyses, nondeteriorated material models were used for the three-story conventional and balanced archetypes, and followed by a second set of analyses on the same archetypes with deteriorated material models. For simplicity, material strain hardening was excluded in both sets of analyses. The resulting pushover curves are compared in Fig. 9. When no strength degradation was considered in the nonlinear model, P-Δ practically has the same effects on both conventional and balanced archetypes, irrespective of seismic weight intensity under consideration [Figs. 9(a and c)]. After reaching their ultimate strength, normalized base shears for archetypes with high and low seismic weight decreased at the same rate in both conventional or balanced design cases.

By contrast, when strength degradation was considered, pushover curves of archetypes designed with high and low seismic weights were significantly different for the conventional design case [Fig. 9(b)], which was not the case for the balanced design [Fig. 9(d)]. For the conventional archetypes, strength degradation occurred in SW320 at 2.2% top story drift, which is more rapid than that in SW320G at 2.5%. Incidentally, the 13% difference between these two starting points of strength degradation is similar to the difference between their CMR values. Regarding the balanced archetypes, both SW320K and SW320GK experienced

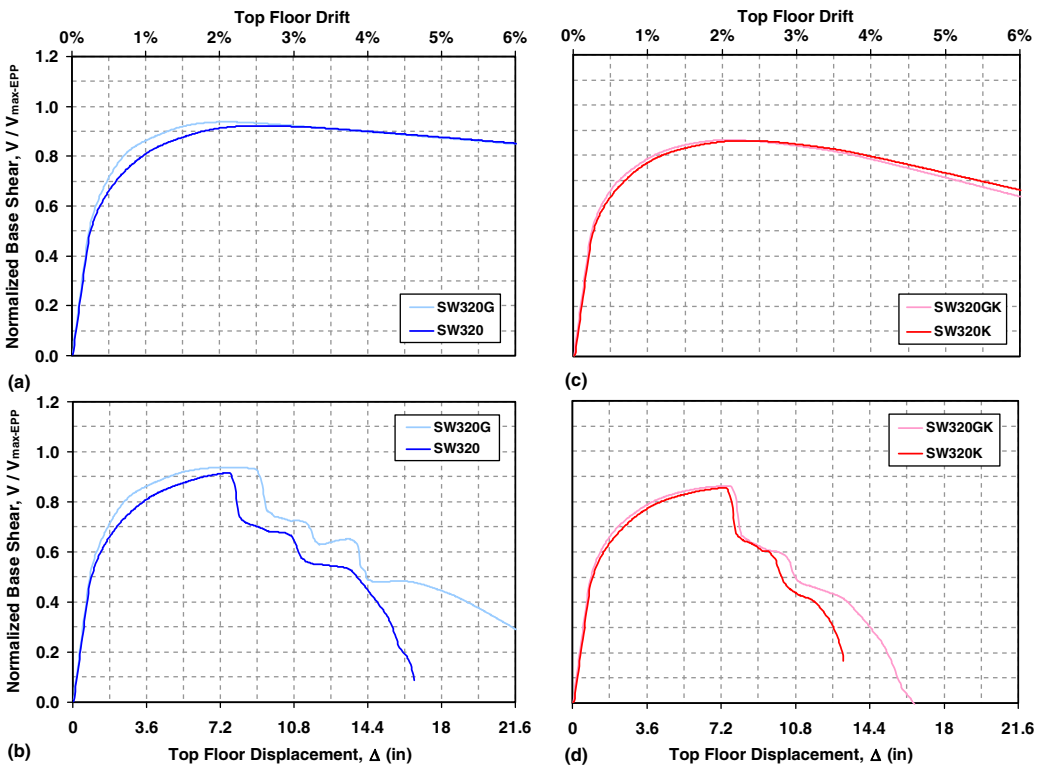

Fig. 9. Seismic weight influence through monotonic pushover analysis on three-story archetypes: (a) 100% design case with deteriorated material model; (b) 100% design case without deteriorated material model; (c) balanced design case with deteriorated material model; (d) balanced design case without deteriorated material model

strength degradation at approximately the same 2.1% top story drift.

Additionally, monotonic pushover analyses were conducted on the five-story conventional and balanced archetypes designed with high and low seismic weight [pushover results are provided by Purba and Bruneau (2014a)]. The same observations reported for the three-story archetypes were evident for the five-story archetypes when no strength degradation was considered in the nonlinear model. Here, P-Δ has practically the same effects on both conventional and balanced archetypes, irrespective of seismic weight intensity. When strength degradation was considered, high seismic weight had a more pronounced impact on the conventional archetypes than on the balanced archetypes. Strength degradation occurred in SW520 at 1.9% top story drift, whereas that in SW520G occurred at 2.4% top story drift. Regarding the balanced archetypes, SW320K and SW320GK experienced strength degradation at approximately 1.8 and 2.2% top story drift, respectively.

Having observed that both the three-story and five-story conventional archetypes designed with low seismic weight exhibited more rapid strength degradation than that with high seismic weight, a subsequent investigation was directed to compare cross-sectional moment capacities of W-sections used for boundary elements of each archetype. As explained in the companion paper (Purba and Bruneau 2014b), during modeling, the moment-rotation relationship at the cross-sectional level was converted into a stress-strain relationship for fibers in an *OpenSees* model using the following equation:

$$\varepsilon = \frac{0.5d \times \theta}{L_p} \tag{5}$$

where ε = fiber strain at the top and bottom of the cross section for pure bending; d = cross-sectional total depth; θ = cross-sectional rotation; and L_p = plastic hinge length ($= 0.9d$). In the absence of axial forces, given that the plastic hinge length is a function of d, the preceding equation simplifies such that the furthest fiber from the neutral axis of any cross section reaches the same strain for a given cross-sectional rotation, irrespective of section depth. For example, to reach the onset of strength degradation at 0.039 rad [Fig. 8 in Purba and Bruneau (2014b)], the furthest fiber from the neutral axis has to reach a strain level of 0.022. However, when axial force is present in a cross section (which is typically the case for boundary elements), the degradation behavior of deep and shallow cross sections will vary because the axial load causes the neutral axis to move away from the center of gravity of the cross section. The larger the axial load, the further the neutral axis shifts away from the center. For shallow cross sections, the strain corresponding to the onset of degradation is reached at a smaller rotation than that in deeper cross sections and strength degradation takes place more rapidly.

As presented in Table 2, cross-sectional depths for the three-story conventional archetypes designed with low and high seismic mass are significantly different. The latter case has relatively larger cross sections. By contrast, this was not the case for the three-story balanced archetypes. Both archetypes designed with low and high seismic mass have comparable sizes of HBEs and VBEs. This explains the results plotted in Fig. 9, in which the strength of the conventional archetype with relatively shallower cross section (i.e., SW320) deteriorated faster than that with a deeper cross section (i.e., SW320G). For the balanced cases (i.e., SW320K and SW320GK), the strength of both archetypes deteriorated at the same time as a consequence of having comparable depth of boundary elements. Hence, the higher CMR values for archetypes designed with high seismic weight are an artifact of the selected boundary element sizes and are not greatly impacted by the P-Δ effect, as initially predicted.

Number of Stories

Another variation in structural configuration considered in this research is the archetype number of stories (or total building height). As a result of different fundamental periods and spectral accelerations at the MCE level, the collapse margin ratio is more likely to vary from one low-rise archetype to another mid-rise archetype. To examine variations in CMR between several archetypes with different numbers of stories, IDA results of the following archetype groups are compared: (1) SW320, SW520, and SW1020; (2) SW320K, SW520K, and SW1020K; (3) SW320G and SW520G; and (4) SW320GK and SW520GK. Their fragility curves and corresponding CMR values are presented in Fig. 7.

In general, CMR increases as the number of stories increases, irrespective of design approaches (i.e., conventional versus balanced design cases) or level of seismic weight intensity (i.e., low versus high seismic weight). However, the CMR increment does not linearly correspond to the increments of number of stories. The results of the first group can be considered as an example. CMR values were 2.40, 2.42, and 4.08 for SW320, SW520, and SW1020, respectively. The less than 1% CMR increase from the three to five stories was not as significant as the approximately 70% increase from the five-story to 10-story archetypes. The same trend was evident for the second group (i.e., balanced archetypes). In addition, whereas CMR discrepancies between the three-story and five-story archetypes in the first and second groups were less than 1%, the CMR discrepancies in their counterpart archetypes (i.e., archetypes in the third and fourth group, which were designed with high seismic weight) were more than 11%.

These results indicate that for the same intensity of ground motions, long-period archetypes have a lower probability of collapsing than short-period archetypes. This finding is similar to examples in FEMA P695 (2009) for both RC special moment frame and wood light-frame archetype systems, in which short-period archetypes had lower values of CMR. In other words, to achieve the same level of collapse margin as long-period archetypes, short-period archetypes for these systems required additional strength or other forms of modification to improve their collapse performance (FEMA 2009).

Recommended Future Research on Seismic Performance Factors

Seismic performance factors (SPFs) for balanced SPSWs have been proposed, and the values currently specified for conventional SPSW have been verified as adequate. These factors were determined from the collapse performance evaluation of several SPSW archetypes designed to consider key structural configurations such as panel aspect ratio, seismic weight intensity level, and number of stories (building height). To further substantiate the proposed SPF for balanced design, considering a larger number of SPSW archetypes may be desirable. In particular, SPSW archetypes designed in different seismic design categories may be examined in this more comprehensive investigation.

Table 3 compares collapse performances for archetypes with different panel aspect ratio, seismic weight intensity level, and building height. Among these structural configurations, building height significantly affected values of the collapse margin ratio. Taller archetypes tend to have higher CMR than shorter archetypes, and variations in CMR values between the two were considerably large, particularly for the conventional archetypes. For example,

CMR values for the shorter and taller conventional archetypes varied from 2.1 to 4.08, whereas those for the balanced archetypes varied from 1.52 to 2.30. This is consistent with trends reported in FEMA P695 (2009) for other types of structural systems. As such, further investigation of the FEMA P695 (2009) procedure may be desirable to elucidate the causes of this trend and to investigate whether SPF (particularly *R*-factor) should vary for SPSWs in the short and long period range.

In this research, SPFs were investigated for conventional SPSWs (designed with $\kappa = 1.0$) and balanced SPSWs (designed with $\kappa = \kappa_{\text{balanced}}$). Although SPFs may be interpolated for other SPSWs designed with $\kappa_{\text{balanced}} < \kappa < 1.0$, further investigation is required to quantify SPFs for other κ factors than those investigated in this research.

An unintended source of overstrength may be also be introduced during the design of SPSWs. For example, selecting uniform columns and beams sizes over several stories is common in engineering practice for construction simplicity. In the SPSW design, structural engineers may select similar VBEs, HBEs, and infill plates over several adjacent stories, some of which may have additional strength beyond that required to sustain loads. In addition, the available minimum hot-rolled plate thickness may be thicker than that required by design, thus providing another source of overstrength to the system (assuming that special perforated SPSW design provisions are not used). The resulting additional overstrength may increase the margin to collapse, which would most benefit the balanced archetypes in this case. Further research may investigate the conditions in which such overstrength can be systematically relied upon to possibly increase the *R*-factor. Finally, as more research on SPSW becomes available, the impact of total system collapse uncertainty and rate of deteriorated material models on SPSW collapse performance can be reassessed.

Conclusions

The seismic performance of SPSWs having infill plates designed by considering two different philosophies (i.e., conventional and balanced designs) was investigated by using the FEMA P695 methodology (2009). All conventional archetypes met the FEMA P695 performance criteria for the *R*-factor of 7 used in their design. The Ω_o factor of 2 and C_d factor of 7 can be considered for conventional SPSWs. The seismic performance factors determined for conventional SPSWs are similar to those specified in ASCE 7-10 (2010) (i.e., *R*, Ω_o, and C_d factors are 7, 2, and 6, respectively). By contrast, the balanced archetypes designed with an *R*-factor of 7 did not meet the FEMA P695 (2009) performance criteria. To rigorously meet the performance criteria, an *R* factor of 5 was required for the balanced SPSWs. No system overstrength factor was available for balanced SPSWs (i.e., $\Omega_o = 1$) and the C_d factor for balanced SPSWs should be similar to the assigned *R*-factor.

Most importantly, the balanced archetypes were found to have a higher probability to suffer significantly larger (and unacceptable) interstory drift than the conventional archetypes. Savings in steel when designing balanced SPSWs with a lower *R*-factor came at the cost of the SPSWs developing much larger interstory drifts than those of the conventional SPSWs under MCE ground motions. These findings suggest that the infill plates of SPSWs should be designed to resist the total specified story shears, rather than to share those forces between the boundary frame and infill.

Acknowledgments

Incremental dynamic analyses were executed using the NEES-HUB supercomputer. This work was supported in part by the George E. Brown, Jr. Network for Earthquake Engineering Simulation (NEES) Program of the National Science Foundation under NSF NEESR Award Number CMMI-0830294. The financial support of the Fulbright Indonesia Presidential Scholarship to the first author is gratefully appreciated. However, any opinions, findings, conclusions, and recommendations presented in this paper are those of the writers and do not necessarily reflect the views of the sponsors.

References

AISC. (2010). "Seismic provisions for structural steel buildings." *ANSI/AISC 341-10*, Chicago.

ASCE. (2010). "Minimum design loads for buildings and other structures." *7-10*, Reston, VA.

Bhowmick, A. K., Driver, R. G., and Grondin, G. Y. (2011). "Application of indirect capacity design principles for seismic design of steel-plate shear walls." *J. Struct. Eng.*, 10.1061/(ASCE)ST.1943-541X.0000303, 521–530.

Bruneau, M., Uang, C. M., and Sabelli, R. (2011). *Ductile design of steel structures*, 2nd Ed., McGraw-Hill, New York.

Canadian Standards Association (CSA). (2009). "Design of steel structures." *CAN/CSA S16-09*, Willowdale, ON, Canada.

FEMA. (2000). "State of the art report on systems performance of steel moment frames subject to earthquake ground shaking." *FEMA Rep. No. 355C*, SAC Joint Venture Partnership for FEMA, Washington, DC.

FEMA. (2009). "Quantification of building seismic performance factors." *FEMA Rep. No. P695*, Applied Technology Council for FEMA, Washington, DC.

OpenSees version 2.0 [Computer software]. Pacific Earthquake Engineering Research Center, Univ. of California, Berkeley, CA.

Pacific Earthquake Engineering Research Center (PEER). (2005). "PEER NGA database." Univ. of California, Berkeley, CA, ⟨http://peer.berkeley.edu/nga/⟩ (Jan. 12, 2012).

Purba, R., and Bruneau, M. (2012). "Case study on the impact of horizontal boundary elements design on seismic behavior of steel plate shear walls." *J. Struct. Eng.*, 10.1061/(ASCE)ST.1943-541X.0000490, 645–657.

Purba, R., and Bruneau, M. (2014a). "Seismic performance of steel plate shear walls considering various design approaches." *Tech. Rep. MCEER-14-0005*, Multidisciplinary Center for Earthquake Engineering Research, State Univ. of New York at Buffalo, Buffalo, NY.

Purba, R., and Bruneau, M. (b). "Seismic performance of steel plate shear walls considering two different design philosophies of infill plates. I: Deterioration model development." *J. Struct. Eng.*, 10.1061/(ASCE)ST.1943-541X.0001098, 04014160.

Qu, B., and Bruneau, M. (2009). "Design of steel plate shear walls considering boundary frame moment resisting action." *J. Struct. Eng.*, 10.1061/(ASCE)ST.1943-541X.0000069, 1511–1521.

Vamvatsikos, D., and Cornell, C. A. (2002). "Incremental dynamic analysis." *Earthquake Eng. Struct. Dyn.*, 31(3), 491–514.